PHYSICAL REVIEW A VOLUME 13, NUMBER 1 JANUARY 1976

Ionization, charge exchange, and excitation in F + Ar and F + Kr collisions*

Forrest Hopkins, Rudiger Brenn,† and Anthony R. Whittemore
Department of Physics, State University of New York, Stony Brook, New York 11794

Nelson Cue and Vince Dutkiewicz
Department of Physics, State University of New York, Albany, New York 12222

R. P. Chaturvedi
Department of Physics, State University of New York, Cortland, New York 13045

(Received 15 April 1975)

We have measured projectile and target x-ray cross sections for F + Ar and F + Kr collisions using fluorine beams of charge states 7+, 8+, and 9+ with energies from 20 to 76 MeV. Pronounced enhancements for the Ar K and Kr L vacancy cross sections using F^{9+} ions compared to those for the 7+ projectile can be explained by charge exchange as described by an empirically scaled Brinkman-Kramers theory. The Ar L, Kr K, and Kr M cross sections are found to exhibit features expected for Coulomb ionization. The projectile K x-ray production for the 9+ ion is accounted for by charge exchange processes. Predictions of the first Born approximation for direct single-step excitation to bound states by the target nucleus overestimate the observed cross sections for F^{7+} and F^{8+}.

I. INTRODUCTION

The complexity and the number of modes of excitation playing major roles in heavy-ion–atom collisions has become evident as the result of several recent experiments. In particular, for asymmetric collisions at MeV/amu bombarding energies, inner-shell vacancy cross sections have been found to deviate substantially from the quadratic dependence on projectile Z suggested by simple Coulomb ionization theories.[1] The experimental evidence has led to modifications of the description of the ionization process itself as well as the consideration of additional mechanisms for creating vacancies. We present in this paper a study of the projectile-charge-state dependence of the x-ray cross sections for collisions involving highly stripped fluorine projectiles with argon and krypton targets. In the analysis of the data, we have considered specifically three mechanisms for the creation of inner-shell vacancies: ionization, charge exchange, and direct Coulomb excitation to bound states within the one- and two-electron projectiles.

The process which has received a majority of recent experimental attention is ionization. Departures from the Z^2 dependence in ionization were first reported for several light projectiles ($Z \leq 3$)[2-4] and subsequently for heavy ions.[4-6] In the regions of $\eta^{1/2}$ [= (projectile velocity)/(orbital electron velocity)] relevant to the present work, two effects have been suggested[4] to account for observed depressions and enhancements in the cross sections below and above $\eta^{1/2} \approx 0.5$, respectively. The former effect involves an increase in the binding energy U_B of the electron due to the presence of the projectile charge within the K shell[4] or the L shell.[7] The $1/U_B^2$ dependence in either the binary-encounter approximation (BEA)[8] or the plane-wave Born-approximation (PWBA)[9] formulations then leads to a reduction in the cross section. The second effect is also based upon a quasiadiabatic adjustment of the bound electron to the projectile charge, in this case a polarization which decreases the interaction distance and so increases the ionization probability. Cancellation of the two effects has been suggested[4] to occur at $\eta^{1/2} = \theta/2$, where θ is the Born screening parameter[1] for the shell being considered. Experimentally, for heavy ions, these crossover points are observed to fall reasonably close to the predicted values.[5,6]

Rather dramatic evidence for the importance of processes other than Z^2 ionization in inner-shell vacancy cross sections has been reported in the strong projectile-charge-state dependence of target x-ray cross sections for $F^{7+,8+,9+}$+Ar collisions[10,11] and for $Ar^{11+-16+}$+Ne collisions.[12] Theoretical estimations of the magnitudes for the F → Ar experiment in terms of charge-exchange cross sections have been made within the BEA[13] and first Born (Brinkman-Kramers)[14] frameworks. More recent and intensive attempts to analyze the charge-state dependence in the F + Ar case with the electron capture mechanism have met with success in the employment of the Brinkman-Kramers cross section advanced by Nikolaev[15] with velocity-dependent scaling based on either the measured total capture[16] or the measured F K x-ray cross section with the F^{9+} ion.[17] It seems

apparent that the inclusion of electron capture in attempts to explain the available experimental results is a promising step toward understanding the many and varied aspects of heavy-ion–atom collisions.

The data and analysis presented in this paper are intended to provide further information on the respective roles of ionization and charge exchange in such collisions. Of particular interest is the applicability of the Nikolaev expression in explanations of charge-state effects, i.e., the consistency and validity of the velocity-dependent scaling. In addition, the topic of Coulomb excitation to bound states was found relevant in the evaluation of the projectile K x-ray cross sections at the higher energies.

II. EXPERIMENTAL PROCEDURES

The fluorine beams with energies from 20 to 76 MeV utilized in this experiment were provided by the Stony Brook FN Tandem Van de Graaff Accelerator. Individual charge states 7+, 8+, 9+ were obtained by inserting a 20-μg/cm^2 carbon foil between the 90° analyzing magnet and the switching magnet preceding the beam line. Where possible, charge states directly from the accelerator terminal were also used. Beam currents on target ranged from ~1 to ~50 nA, depending on availability and counting rates.

The target cell consisted of a doubly differentially pumped gas cell as diagrammed in Fig. 1. Four apertures sequentially positioned along the beam axis with diameters 1.5, 2.0, 2.5, and 3.0 mm (alternatively 3.5 mm), respectively, provided both beam collimation and graduated pumping regions. The center target chamber, defined by the second and third apertures, was 1.0 cm in length. The intermediate region, ~5 cm in length on either side of the target region, was tied directly into a 1500-l/sec diffusion pump. Pumping for the beam line preceding the cell and the beam dump was provided by two 220-l/sec turbopumps. Argon and krypton gases were introduced into the target region by means of an electronic leak valve. Through a separate port on the same region, the pressure was monitored with a Baratron capacitance manometer. Control of the gas flow and pressure was accomplished either automatically with a leak-valve–manometer feedback or by simply setting a pressure and keeping a careful check on pressure drift.

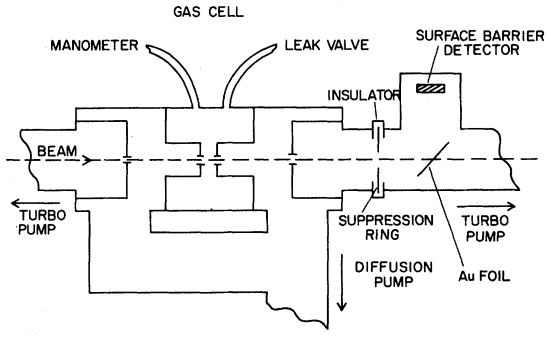

FIG. 1. Diagram of doubly differentially pumped gas cell.

Two detectors were used simultaneously to detect x rays. An 80-mm^2 Si(Li) detector with a 1-mil Be entrance window was placed on one side of the cell at 90° to the beam axis to record Ar K, Kr K, and Kr L lines. The Si(Li) was used alternately either coupled directly into the gas cell or placed outside of a 0.00125-cm-thick Mylar window capping the cell. Opposite the Si(Li) detector and vacuum coupled into the system to detect Ar L, Kr M, and F K x rays was positioned a center-wire flow proportional counter[18] operated at 2100 V with a 10%-methane–90%-argon gas mixture. Both detectors were provided with various collimating apertures. The entire 1.0-cm active path length was visible to the Si(Li). A rectangular aperture was employed to shield the stainless steel apertures from the proportional counter so as to eliminate projectile x rays from sources other than the target gas. Typical solid angles subtended were 6.9×10^{-3} and 4.0×10^{-3} sr for the former and latter, respectively. Energy calibration was accomplished with a ^{55}Fe source which could be inserted into the evacuated target region. Resolution of the Si(Li) was typically 210 eV for the 5.9-keV Mn $K\alpha_{1,2}$ x ray, while the proportional counter had an intrinsic resolution of ~25% for the Mn line.

Beam integration was accomplished two ways. The first was integration with a calibrated current integrator of the charge collected in the beam dump, which was preceded by a ring biased to −300 V. The second, and the method used most often, was recording Rutherford scattering at 90° from Au foils of known thicknesses located in the first part of the beam dump approximately 15 cm from the exit (fourth) aperture of the gas cell. The Au thicknesses (300–400 μg/cm^2) were determined from energy loss[19] of the fluorine ions at several incident energies. The charge integration was in rough agreement with the elastic scattering but was found to be sensitive to changes in the pressure in the beam dump. Consequently the more reliable elastic scattering values were used in the data reduction. The solid angle for the surface barrier detector at 90° was 5.1×10^{-4} sr.

A most important part of all of these runs was the assurance of single-collision conditions, i.e., charge-state purity of the beam. The linearity of x-ray production with changes in target pressure was checked for various energies. Typical results are shown in Fig. 2. Data points were always taken well within single-collision regions of pressure. All of the Ar and Kr runs were taken at ~10-μ target pressure, with resulting pressures of ~0.2 μ and ~2×10^{-6} torr in the intermediate region and beam line/beam dump, respectively. Residual pressure in the active region was 0.1 μ and was due primarily to leakage through the 2-μm Makrofoil window of the proportional counter.

Data were taken in the form of 1024-channel spectra for the Si(Li) and 256-channel spectra for both the proportional counter and particle detector. Prior to the analog-to-digital conversion, the pulses from all three detectors were self-gated via single-channel analyzers (SCA) set to reject noise and saturated pulses. A dead-time reading was derived from a comparison of the number of the SCA pulses to the number of signals digitized in the multiplexed ADC. Counting rates were kept sufficiently low to ensure deadtimes of at most a few percent. All of the spectra were stored on magnetic tape for subsequent analysis.

Extraction of yields for the Ar K, Kr K, and Kr L x rays in the Si(Li) spectra involved integration of photopeak areas with subtraction of a linear background determined by best-fit procedures. Also the centroids of the Ar $K\alpha$ and $K\beta$ components were obtained from a least-squares fitting of two

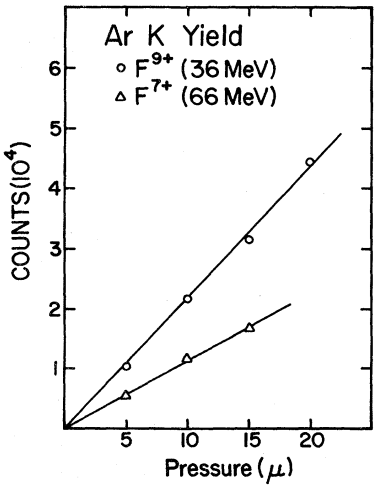

FIG. 2. Typical pressure curves for Ar K x-ray production.

Gaussians plus a linear background, for the purpose of estimating K fluorescence yields. Extraction of yields from the proportional-counter spectra required in each case a least-squares fitting of two Gaussians corresponding to the F K and either the Ar L or Kr M superimposed on an exponential tail representing electronic noise. Spectra taken at several energies with the target gas removed revealed very small backgrounds in the spectra, negligible for the Si(Li) and at most 5% for the proportional counter in the region of interest. Fitting errors were significant only for the proportional-counter spectra, around 10% for the F K lines and 20% for Ar L and Kr M x rays.

Cross sections were determined from the expression

$$\sigma_x = N/t\phi\Omega\epsilon\,, \tag{1}$$

where N is the number of observed x rays corrected for dead-time loss, t is the target thickness (3.53×10^{14}/cm^2), ϕ is the total number of beam particles, Ω is the solid angle subtended by the detector, and ϵ is a correction for absorption. The absorptions of Ar K, Kr K, and Kr L x rays in the Be window of the Si(Li) were taken from the manufacturer's efficiency curve.[20] The transmission through the 2-μm Makrofoil of the F K, Ar L, and Kr M x rays was measured simply by repeating several runs with a second foil inserted between detector and target. Average values of 0.32, 0.38 and 0.42 were obtained for the F K x rays produced with charge states 7+, 8+, and 9+, respectively, matching up well with published values[18] for the 2-μm foil. A value of 0.28 was used for the Ar L and Kr M x rays. It must be stated that increases in the energies of the Ar L and Kr M x rays due to multiple ionization could easily extend part of the lines above the C K absorption edge, where nearly total absorption would occur through just one foil thickness. The determination of the relative importance of that absorption is not possible in the present experiment. Consequently the Ar L and Kr M cross sections must be regarded as tentative. The cross sections for the Kr M x rays must further be regarded as approximate owing to the great variance in the possible energies, which results in additional uncertainties in the absorption corrections. Absolute errors are estimated to be 15% for the Ar K, Kr K, and Kr L cross sections and 20% for the F K x rays. Relative errors should be considerably smaller. For all cross sections isotropic emission has been assumed. Recent measurements[21] indicate strong polarization of F K x rays arising from $F^{7+,9+}$+Ar collisions at and below 33 MeV. The current F K cross sections may be overestimated by as much as 15% owing to the assumption of isotropy.

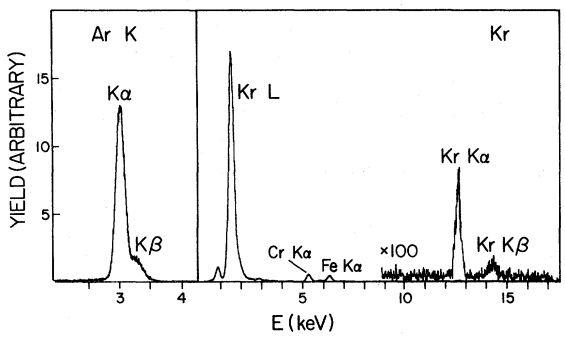

FIG. 3. Spectra with Si(Li) detector of Ar K, Kr K and Kr L x rays.

III. RESULTS

Typical Si(Li) spectra of the Ar K, Kr K, and Kr L x rays with F^{9+} bombardment at 46 MeV are shown in Fig. 3. Proportional-counter spectra for the same beam incident on Ar and Kr are presented in Fig. 4. The energy calibration for the latter is only approximate and is based on the assumption that the centroid of the F K peak is equivalent to the 827-keV energy of the 1s-2p transition in hydrogenic fluorine. High-resolution spectra of the fluorine x rays following capture by 34.8-MeV F^{9+} in Ar indicate that the majority of the x rays belong to that term member.[22]

The measured x-ray cross sections are presented in Tables I and II for Ar and Kr, respectively. Decreasing cross sections coupled with the electronic noise tail precluded accurate determination of the Ar L cross sections above 61 MeV. These data are presented in graphic form in Figs. 5 and 6. The present values are within 20% of the previous data available for the Ar K[11] and Kr L[23]

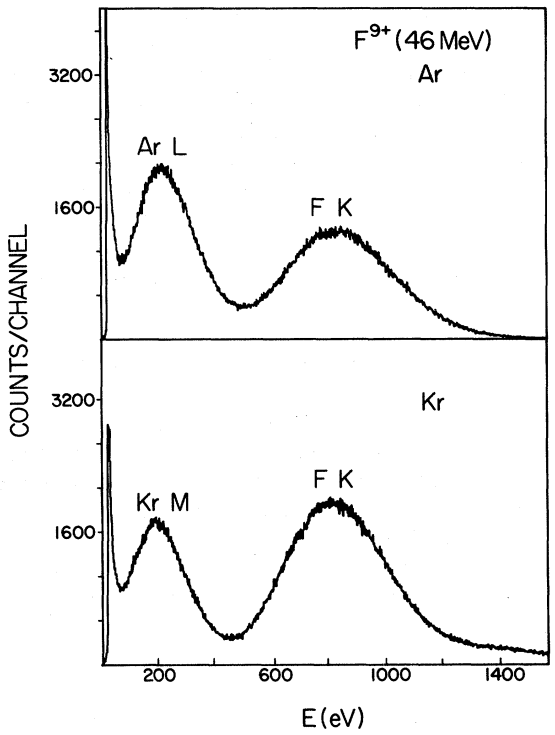

FIG. 4. Proportional counter spectra for Ar and Kr.

shells at F energies at and below 36 MeV. A striking feature of the data is the similarity between the Ar L and Kr M cross sections as well as between the F K cross sections for the two targets.

The peak labeled Ar L in Fig. 4 may include F L x rays produced following capture or excitation. The more energetic of such transitions within one- and two-electron fluorine ions approach[24] ~200 eV and would be unresolved from the Ar L x rays. The energies of the normal Ar L lines

TABLE I. X-ray cross sections for F-Ar collisions.

E	Ar K (10^{-20} cm^2)			Ar L (10^{-18} cm^2)			F K (10^{-18} cm^2)		
(MeV)	9+	8+	7+	9+	8+	7+	9+	8+	7+
20	2.79	1.39	0.75	31.75	18.14	10.80	50.08	12.24	4.94
26	6.55	3.10	1.38	22.50	14.81	9.07	34.54	8.61	4.12
31	9.09	4.65	2.37	16.42	12.65	8.91	23.70	7.03	4.64
36	9.98	5.61	2.75	14.08	10.40	7.05	16.45	5.26	4.23
41	11.93	7.01	3.75	11.44	9.30	6.51	12.89	4.82	4.62
46	14.94	8.08	4.76	10.93	7.94	5.40	10.61	3.82	4.70
51	16.21	9.22	5.43	9.43	7.00	4.94	8.02	3.92	4.72
56	17.79	9.99	5.87	8.20	6.09	4.40	6.37	3.78	4.38
61	18.12	10.65	6.02	6.76	5.50	3.82	5.14	3.56	4.14
66	18.05	10.98	5.88	•••	•••	•••	3.92	3.27	3.93
71	17.08	10.61	•••	•••	•••	•••	2.83	3.03	•••
76	17.09	10.61	•••	•••	•••	•••	2.42	2.58	•••

TABLE II. X-ray cross sections for F-Kr collisions.

E	Kr K (10^{-22} cm^2)			Kr L (10^{-19} cm^2)			Kr M (10^{-17} cm^2)			F K (10^{-18} cm^2)		
(MeV)	9+	8+	7+	9+	8+	7+	9+	8+	7+	9+	8+	7+
26	0.45	0.46	0.47	2.92	1.60	0.90	2.90	1.49	1.01	51.70	10.92	5.71
36	2.25	1.77	1.59	3.69	2.12	1.39	2.22	1.26	0.87	30.60	7.88	6.44
46	5.52	4.86	4.29	3.20	2.23	1.59	1.41	0.97	0.75	14.42	5.77	7.18
56	12.43	9.96	9.39	2.99	1.98	1.78	1.08	0.67	0.62	8.39	4.55	7.73
66	21.13	16.88	16.15	2.51	1.77	1.53	0.93	0.58	0.50	5.14	4.44	6.81
76	33.00	28.91	•••	2.21	1.72	•••	•••	•••	•••	3.97	4.00	•••

are around[25] 220 eV but are expected to be shifted higher here owing to simultaneous M-shell ionization. The transitions to $n=2$ in the F ion following capture into $n>2$ states are expected to be more prolific when the K shell is filled, since all of the decay is via L transitions. Thus if the capture rate into the $n>2$ states is the same for both F^{7+} and F^{9+}, the F L x-ray yield would be larger for F^{7+}, which is contrary to observation. Second, according to theory[15] the F L x-ray yield following capture should exhibit a velocity dependence very similar to that of the F K cross section with F^{9+}. Again our observation does not reflect this behavior. Consequently the assignment of the peak entirely to Ar L x rays is a reasonable one. Similar arguments can be made for the Kr M data.

The conversion of the Ar and Kr x-ray cross sections to vacancy-production cross sections necessitated certain assumptions about the fluorescence yields. The critical dependence of the fluorescence yield for a vacancy in a given shell upon the degree of multiple ionization of the neighboring

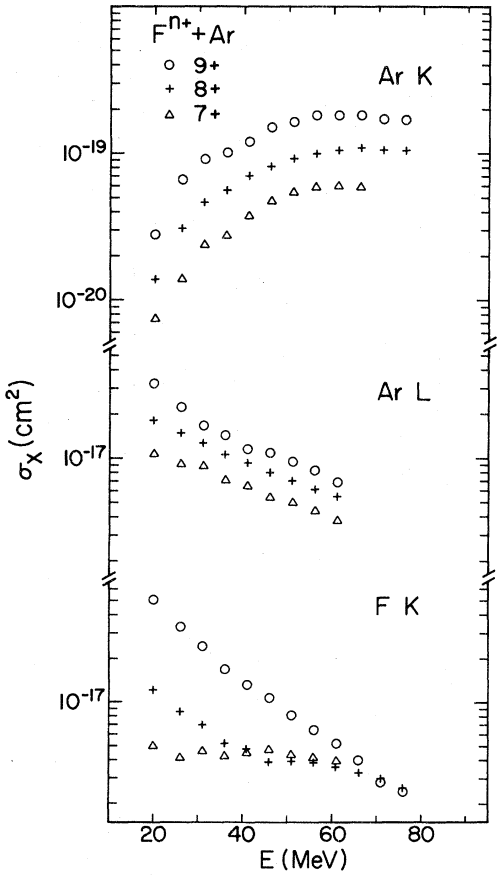

FIG. 5. Ar K, Ar L, and F K x-ray cross sections for $F^{7+,8+,9+}$ bombardment.

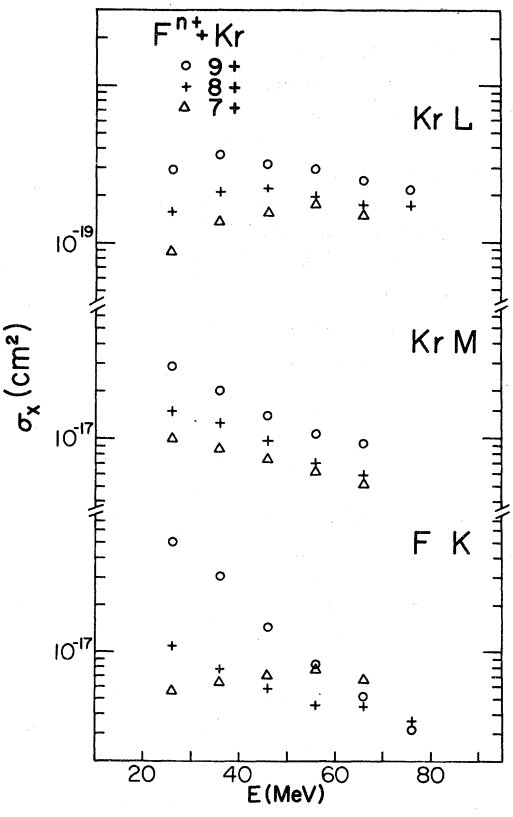

FIG. 6. Kr L, Kr M, and F K x-ray cross sections for $F^{7+,8+,9+}$ bombardment.

outer shell has been well documented experimentally for the K fluorescence yields for neon bombarded by oxygen[26] and chlorine[27]. For the Ar K shell, we have used a single theoretical yield ω_k based on the calculations by Bhalla[28] and on the average degree of ionization indicated by the energy shifts of the Ar $K\alpha$ and $K\beta$ x rays for F^{9+} at 46 MeV. The respective shifts of 65 and 148 eV corresponded to the value 0.146 for ω_k, and can be attributed to various defect configurations involving a total of 6 to 7 vacancies in the $2p$ and $3p$ shells. The fluorescence yields for the other charge states and energies, again based on the energy shifts, fell within ±10% of this number. A recent measurement[29] of Ar K fluorescence yields for 30-MeV F has revealed that such an approach is reasonably accurate.

Owing to a lack of similar information for the Ar L-shell fluorescence yields and further an inability to determine accurately defect configurations from the proportional-counter spectra, we have simply normalized the Ar L x-ray cross section for F^{7+} to the predictions of the binary-encounter approximation (BEA)[8] for ionization using values for the universal function G from McGuire and Richard.[30] Two considerations would suggest that the measured Ar L cross sections, with the exception of the first two of the F^{9+} data points, are essentially due to ionization. Both of these will be discussed more completely in Sec. IV. Briefly, the Ar L vacancy cross section due to capture is expected to behave like the F K x-ray production cross section. The latter is seen to be rapidly decreasing with increases in energy, whereas the observed Ar L yields are well described by the theoretical ionization curve presented in Sec. IV. Second, the empirical scaling of the Brinkman-Kramers expression[15] to be discussed shortly gives a charge-exchange contribution to L vacancy creation which is a small fraction, ~10%, of the BEA ionization curve. The BEA curve is expected to be a reasonable lower limit on the actual ionization taking place, since the Ar L cross section for 600-keV proton bombardment is within 25% of the BEA prediction.[31] Accordingly we have used a single value of $(3.1\times10^{-2})^{-1}$ to normalize the x-ray data to the theory. Theoretical fluorescence yields for the Ar L shell which approach this value have been reported[32,33] and correspond to configurations with nearly fully stripped M shells.

Specific theoretical calculations of the types for the Ar K shell do not currently exist for the Kr K and L shells. Consequently we have used the single average values of 0.66 for the Kr K[34] and 0.024 for the Kr L[35] yields. The former should be accurate for the present case since the $K\alpha$ and $K\beta$ line shifts are observed to be small. For the Kr L shell a comparison with the aluminum K shell, which has a comparable binding energy and atomic fluorescence yield, is instructive. A high-resolution study[36] of the Al $K\alpha$ satellite structure resulting from fluorine bombardment implies that in the present situation the atomic value should be about $\frac{2}{3}$ the actual value at F energies around 36 MeV. Presumably above that energy, it should be even closer owing to decreasing M-shell ionization.

Using the various fluorescence yields discussed above, the vacancy cross sections have been derived from the x-ray data and are presented in Tables III and IV for Ar and Kr, respectively.

IV. DISCUSSION

In order to place emphasis upon the processes involved, we discuss together those cross sections for both the argon and krypton targets thought to reflect a particular process, e.g., ionization and effects associated with it. Included in the category of ionization are the Ar K and Kr L cross sections for F^{7+} and all of the Ar L, Kr K, and Kr M cross sections. The enhancements in the Ar K and Kr L cross sections for the fully stripped F over those for the two-electron F are examined in terms of charge exchange to the K shell of the projectile, along with the F K cross sections for F^{9+}. Finally the projectile x-ray production for incident one- and two-electron F ions receives attention under the heading of excitation.

A. Ionization

As mentioned earlier, the subject of ionization has received a major part of the experimental and theoretical efforts in the area of vacancy cross sections for ion-atom collisions. Of particular interest for the present experiment is the role of

TABLE III. Ar vacancy cross sections.

E	Ar K (10^{-19} cm^2)			Ar L (10^{-16} cm^2)		
(MeV)	9+	8+	7+	9+	8+	7+
20	1.92	0.952	0.517	10.24	5.85	3.48
26	4.52	2.12	1.16	7.19	4.77	2.93
31	6.27	3.19	1.63	5.30	4.08	2.87
36	6.88	3.84	1.90	4.54	3.35	2.27
41	8.23	4.80	2.59	3.69	3.00	2.1
46	10.3	5.53	3.28	3.53	2.56	1.74
51	11.2	6.32	3.74	3.04	2.26	1.59
56	12.2	6.84	4.05	2.65	1.96	1.42
61	12.4	7.30	4.15	2.18	1.77	1.23
66	12.4	7.52	4.06	...	...	...
71	11.7	7.27	...	...	...	...
76	11.7	7.27	...	...	...	...

TABLE IV. Kr vacancy cross sections.

E (MeV)	Kr K (10^{-22} cm^2) 9+	8+	7+	Kr L (10^{-18} cm^2) 9+	8+	7+	Kr M (10^{-16} cm^2) 9+	8+	7+
26	0.676	0.696	0.718	12.2	6.68	3.74	30.3	15.6	10.5
36	3.40	2.67	2.41	15.4	8.82	5.80	23.1	13.2	9.09
46	8.37	7.37	6.50	13.3	9.30	6.63	14.7	10.1	7.85
56	18.8	15.1	14.2	12.5	8.31	7.41	11.2	7.27	6.49
66	32.0	25.6	24.5	10.5	7.37	6.40	9.74	6.09	5.28
76	50.0	43.9	...	9.21	7.15	...	...	...	...

"finite charge effects" suggested to account for the substantial departure from Z^2 dependence observed previously in the ionization of various target K shells by heavy projectiles.[4-6]

The Ar K vacancy cross sections for F^{7+} bombardment are shown in Fig. 7 compared to a BEA ionization curve, which has been normalized to a scaled (×81) proton cross section at 3.0 MeV/amu. The F^{7+} cross sections divided by the product of Z^2 (=81) and the proton cross sections at identical projectile velocities from Winters *et al.*[37] are shown in Fig. 8; also in which the prediction for the scaled cross sections including the "increased-binding" effect[3] is presented. The data reach a crossover point somewhat above the $\eta_k^{1/2} = \theta/2$ value but do dip toward the binding curve for $\eta_k^{1/2} < 0.5$. Both of these characteristics have been noted before[6] for similar projectile-target combinations. In line with considerations discussed in the following sections, the strength of the electron capture from the Ar K shell to $n \geq 2$ states in F is expected to be small compared to ionization. The data here indicate that such is the case.

The Ar L vacancy cross sections displayed in Fig. 7 exhibit a velocity dependence which is well described by the binary-encounter approximation. The arbitrary normalization by $(3.1 \times 10^{-2})^{-1}$ precludes any accurate comparison of magnitudes. A reasonable expectation based on available information on heavy-ion ionization cross sections for $\eta^{1/2} > 0.5$ is that the Z^2 scaled BEA curve is an

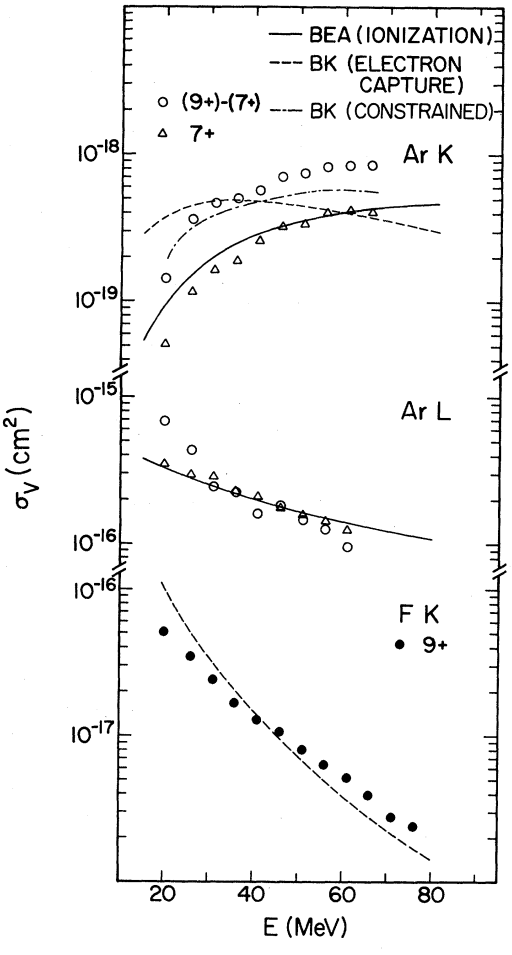

FIG. 7. Ar K and Ar L vacancy cross sections in terms of F^{7+}-induced magnitudes and the (9+) − (7+) differences. Included is the F K x-ray cross section for F^{9+} (see text for details of theoretical curves).

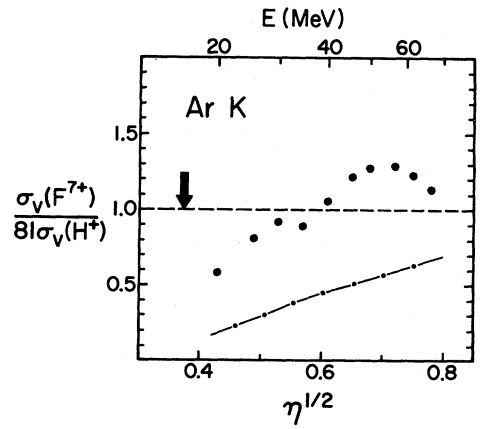

FIG. 8. Proton-scaled Ar K vacancy cross section for F^{7+} compared to increased-binding prediction (dot-dashed curve). The arrow indicates $\eta_k^{1/2} \approx \theta/2$.

underestimate of the actual cross section, although no such measurements exist for a shell as loosely bound (~245 eV) as the Ar L shell.

The charge-state dependence in the Ar L cross sections is comparable to that expected for ionization due to ionic charge (full screening) rather than nuclear charge. Two recent experimental papers have interpreted their results in terms of screening effects. The first[28] noted a partial screening due to Cl L electrons as reflected in the Ne K vacancy cross sections for Cl-Ne collisions. The second[38] reported that ionization of the Ne L shell simultaneous with the creation of Ne K vacancies, observed in the Ne $K\alpha$ satellite structure, appeared to be due to the ionic charge of C, N, O, and F projectiles. The latter case is relevant to the situation here, where the projectile electrons are considerably more tightly bound than the target electrons. A full screening assumption here predicts an increase of 65% for F^{9+} compared to F^{7+}, close to the observed differences in Fig. 7. The first two F^{9+} data points depart somewhat from the behavior of the remaining Ar L cross sections, possibly owing to Ar L x rays arising from capture as discussed previously. It must be kept in mind that the same normalization of $(3.1 \times 10^{-2})^{-1}$ has been applied to all of the data points. Thus the 9+ values for the vacancy cross sections may be overestimated somewhat with respect to the other values, as the "average" fluorescence yield might be expected to be larger for the fully stripped ion.

The vacancy cross sections for the Kr K shell in Fig. 9 show little charge-state dependence up to $\eta_k^{1/2} \approx 0.4$, as has been observed before at lower energies.[39] The proton-scaled[37] cross sections in Fig. 9 again, as in the Ar K case, exhibit trends expected for ionization, tracking the appropriate increased binding curve[3] at low $\eta_k^{1/2}$. Using scaling discussed in Sec. IV B, charge exchange from the Kr K shell should be down at least a factor of 10 from the measured cross sections, in agreement with the small dependence on charge state.

The Kr L cross section for F^{7+} along with the Kr M cross sections for F^{7+} and the differences between F^{7+} and F^{9+} are shown in Fig. 10. The BEA ionization curve for the L shell has been normalized to a measured proton cross section[37] at 3.0 MeV scaled up by 81, while for the M shell the curve is purely theoretical, using 213 eV for an average binding energy. The normalization value of $(1.2 \times 10^{-1})^{-1}$ for the M shell includes the absorption uncertainties mentioned previously for the M x rays as well as those introduced by assuming a single M binding energy. The intent here is simply to point out the agreement between the measured velocity dependence and the theory.

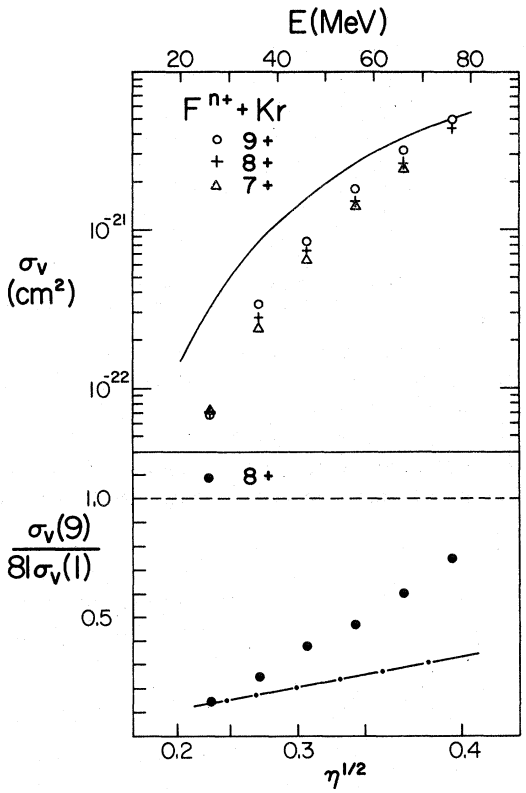

FIG. 9. Kr K vacancy cross sections compared to BEA curve and to increased-binding correction for proton-scaled values (arrow at $\theta/2$).

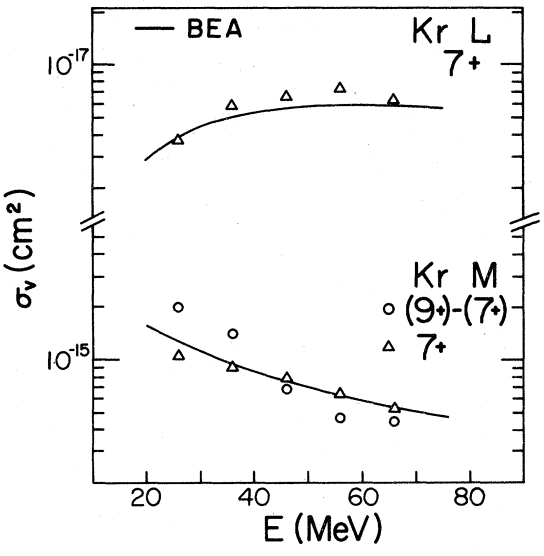

FIG. 10. Kr L and Kr M F^{7+}-induced vacancy cross sections and the (9+)−(7+) difference for Kr M, compared to predictions for ionization.

Within these velocity regions, $0.66 \leq \eta_L^{1/2} \leq 1.05$ and $1.88 \leq \eta_M^{1/2} \leq 3.0$, the ionization description appears adequate. The Kr M cross sections bear features almost identical to those of the Ar L data, not surprising in view of the closeness of the Kr M and Ar L binding energies.

B. Charge exchange

The Brinkman-Kramers (BK) treatment[40] of the simple $-e^2/r$ interaction within a first-Born-approximation framework was generalized by Nikolaev[15] to give the following expression for electron capture by a bare projectile into states with principal quantum number n from a filled target shell of principal number n_i:

$$\sigma(n_i/n) = \pi a_0^2 (\tfrac{256}{5}) N_i n^2 (v_0/v)^2 \gamma^5 \eta_n^5 f(\beta\gamma) . \qquad (2)$$

Here $a_0 = \hbar^2/e^2$, $v_0 = e^2/\hbar$, N_i is the number of electrons in the target shell, v is the projectile velocity, and η_n is the ratio of the orbital electron velocities for states n and n_i. γ is a simple function of η_n and the quantity $V = v/u$, where u is the electron velocity for the state n_i, while f is a function of γ and a screening parameter β. The expression assumes identical "average" parameters to describe subshells within a target shell and includes a sum over final states.

As noted by Nikolaev, empirical scaling of the magnitude of the cross section is required if agreement with experimental data for protons incident on a variety of gases is to be obtained. A similar need for scaling of the total capture cross sections for heavy fully stripped projectiles has been reported.[41,42] More recently velocity-dependent scaling has been used successfully[16] to account for the projectile-charge-state dependence in the Ar K vacancy cross sections with $F^{7+,8+,9+}$ impact, below 36 MeV.

The results of using a velocity-dependent scaling are compared with the differences between the F^{9+} and F^{7+} cross sections in Fig. 7 for the Ar K shell and in Fig. 11 for the Kr L shell. The corresponding F K x-ray cross sections for incident F^{9+} are also displayed for completeness. Assuming that the ionization of the target is nearly the same for F^{9+} and F^{7+}, i.e., minimal screening effects, the cross-section difference should just reflect the charge-exchange contribution from either Ar K or Kr L to the F K shell. According to Eq. (2), this component forms 80–90% of the capture cross sections from either one of these target shells. The dashed curves are the predictions of Eq. (2) using constant scaling factors of 0.11 and 0.05, respectively, for Ar K and Kr L. Capture to the $2S_{1/2}$ metastable state has been excluded. In each case, normalizing the dashed curve for F K x rays to the measured values results in a corresponding adjustment of the dashed curve for the target. The results are shown as a dot-dashed curve for Ar and as a solid curve for Kr. The new predictions in both cases are seen to reproduce the magnitude to within 50% at worst. More striking are the reproductions of the observed velocity dependences. In the case of the Ar K shell, the adjusted curve tracks data which is increasing up to $\eta_k^{1/2} \approx 0.8$, well above the point at which the direct BK curve starts receding. The agreement is somewhat surprising since the particular components are only a fraction of the total capture cross sections. The Kr L-shell to the F K-shell component is only ~9% at 26 MeV, increasing to ~30% at the higher energies. The Ar K to F K process is less than 1% of the total. The lack of better agreement in both cases may just reflect misestimation of the experimental (9+) – (7+) magnitude owing to the use of a single fluorescence yield and to neglect of the screening by the F K electrons in ionization.

The similarity of the scaling factors for the Ar and Kr targets can be seen in Table V. The factors for protons are around 2 times larger at equivalent velocities.[15] The principal shells involved in the total cross section for capture as well as for pro-

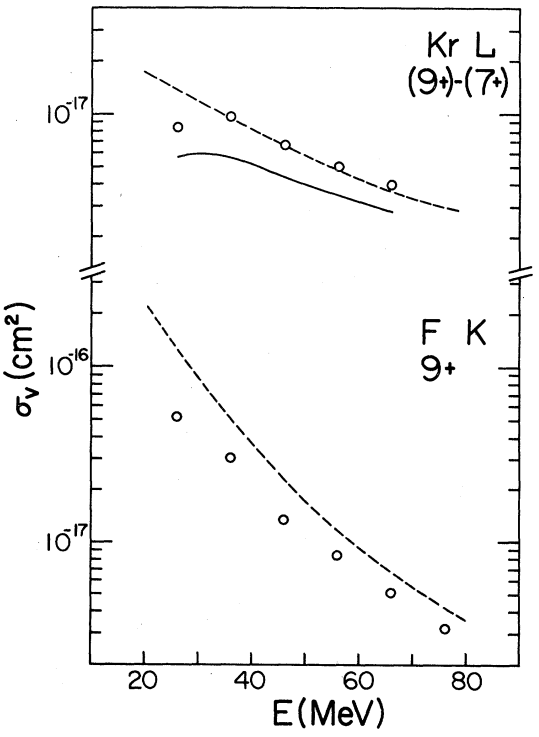

FIG. 11. (9+) – (7+) differences for Kr L vacancy cross sections with single scaled (dashed) and multiply scaled (solid) BK curves.

jectile K x rays are in each case filled, making negligible the corrections[15] for the partially filled outermost target shells. The scaling factor is known to decrease still further for energies below those in Table V.[42] In spite of the larger F nuclear charge and the possibility of "finite charge effects" such as those discussed above for ionization, the success of simple scaling is remarkable in that one normalization at each energy accounts for processes of grossly differing dynamics, i.e., capture from inner shells versus capture from outer shells. Inasmuch as the inadequacy of the theory in explaining the impact-parameter dependence of the Ar K cross section using F^{9+} has been reported,[43] the fact that the theory works as well as it does for estimating total cross sections is an intriguing result.

C. Excitation to bound states

The subject of Coulomb excitation to bound states, as opposed to the continuum (ionization), has been dealt with by numerous theoretical papers.[44] Although data for collisions involving excitation of hydrogen, helium, and outer shells of heavier particles are available,[45] the subject has escaped definitive study as far as experimentation with the inner shells of heavy ions is concerned. Presumably the difficulty lies in distinguishing the process from other possible mechanisms for creating inner-shell vacancies. The use of few-electron F projectiles in the present experiment affords a qualitative look at this mechanism, insofar as some estimate of competing processes in producing F K x rays can be made.

For example the F K x-ray cross sections for F^{8+} incident on Ar appear to reflect different processes at different energies. At the lower energies the data mimic the cross section for F K x rays following capture by F^{9+}. Above 41 MeV, it assumes the shape and nearly the magnitude of the F^{7+} data points, which ostensibly represent some form of excitation of at least one K-shell electron. It seems reasonable to assume that the capture contribution to the 8+ cross section above 41 MeV is roughly in the same proportion to the F^{9+} cross section as at the three lowest energies, that is, down by a factor of ~4. Thus it is informative to compare the F^{8+} cross sections above 56 MeV with expectations for Coulomb excitation. The F^{7+} data can likewise be compared to excitation for a two-electron ion. It must be kept in mind that this is a qualitative assessment in that available high-resolution data[21,46] for F incident on a variety of gases indicate that multistep events are highly probable. Two such possibilities leading to F K x rays are electron exchange and ionization of the F K shell coupled with capture into the F L shell.

TABLE V. Scaling factors for BK charge exchange cross sections based on F K x-ray cross sections F^{9+}.

E (MeV)	Ar	Kr
20	0.05	•••
26	0.07	0.054
31	0.077	•••
36	0.081	0.078
41	0.096	•••
46	0.113	0.080
51	0.119	•••
56	0.129	0.088
61	0.141	•••
66	0.141	0.094
71	0.130	•••
76	0.144	0.118

Bates has noted[44] that within the first born approximation Coulomb excitation from ground state a to an excited state b within a hydrogenic system is given by

$$\sigma(a,b\,|\,Z_1,Z_2,M_2,E)=(Z_1^2/Z_2^4)\sigma(a,b\,|\,1,1,1,E/M_1Z_2^2)\,. \tag{3}$$

Here Z_1 and Z_2 are projectile and target nuclear charge, respectively, and $\sigma(a,b\,|\,1,1,1,E/M_1Z_2^2)$ is the cross section for exciting the hydrogen atom from the ground state a to the state b by proton bombardment. Dividing out the dependence on Z_1 and Z_2 leaves a single "universal curve" for excitation analogous to that[1] for ionization, differing only in that b is a bound state rather than continuum states, against which experimental results for different projectile-target combinations can be tested. We have used closed-form expressions for the proton-hydrogen excitation from Van den Bos and deHeer[47] in obtaining the theoretical curve shown in Fig. 12. The $\sigma(1s\rightarrow 2p)$ and $\sigma(1s\rightarrow 3p)$ cross sections have been added to give σ_T, with higher terms of smaller magnitude neglected. The use of one-electron F provides a hydrogenic "target" as well as opening up completely the excitation channel with the highest probability, $\sigma(1s-2p)$, according to Eq. (3).

The F K x-ray cross sections, as shown in Fig. 10 for F^{7+} incident on Ar and Kr, and the higher-energy F^{8+} ions on Ar, have been multiplied by the factor (Z_2^4/Z_1^2n), where n is the number of F K electrons, $Z_2=9$, and $Z_1=18$ or 36. For the assumption of bare charge for the neutral Ar and Kr projectiles, there is an overestimation of all cross sections. Allowing for full screening due to the Ar K and Kr K and L electrons, all more tightly

bound than the F K electrons, still places the measured data points below the first Born curve by a factor of 3. It should be pointed out that the x-ray cross sections for F^{7+} underestimate the excitation in that only ~30% of the $1s\text{-}2p(^3P_1)$ metastable states formed (lifetime[48] of 0.534 nsec) decay in the viewing region. It is known[21] that at 36 MeV a large fraction of the total excitation goes to that state, in spite of its being a forbidden one-step spin-flip transition.

The reasons for the discrepancies are not currently known. In any case, the above comparisons indicate that Eq. (3) serves as a guide in estimating excitation cross sections, specifically upper limits for those situations where Coulomb excitation is thought to dominate.

V. SUMMARY

The single-collision measurements performed here have allowed us to delineate regimes in which various of the mechanisms responsible for inner-shell vacancy production appear to dominate. In our analysis of the observed strong projectile-charge-state dependence in σ_v for Ar K and Kr L we have found that an empirically scaled Brinkman Kramers treatment of charge exchange as generalized by Nikolaev provides a surprisingly good reproduction of the enhancement of those cross sections for F^{9+} impact over those for F^{7+} impact. The scaling factors used, which were based on the measured F K x-ray cross sections, are found to be of about the same magnitude for both Ar and Kr.

The corresponding exchange implied for the Ar L, Kr K, and Kr M shells is reduced from cross sections expected for ionization of those shells. The absolute magnitudes, velocity dependences, and charge-state dependences of the measured vacancy cross sections are compatible with that picture.

Significant projectile K x-ray yields have been observed for one- and two-electron ions, even at higher velocities where charge exchange as gauged by the F^{9+} results has declined. Calculations of direct Coulomb excitation of K electrons to bound states based on the first Born approximation substantially overestimate the experimental x-ray cross sections.

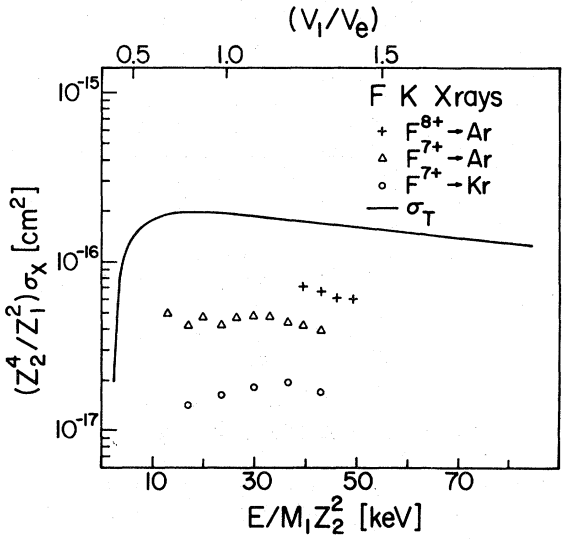

FIG. 12. F K x-ray cross section f for F^{7+} and F^{8+} compared to universal curve for Coulomb excitation to bound states from the first Born approximation.

Thus many of the seemingly complex features of the asymmetric collisions discussed in this paper can be interpreted fairly successfully within a first-order framework, i.e., PWBA or BEA. Allowances for screening in ionization and velocity-dependent scaling of the BK theory provide a useful first basis for examining the origin of the various charge-state effects. The possibilities of second-order effects, i.e., "finite charge effects", and alternative mechanisms, such as excitation and exchange from molecular-orbital processes,[49] invite further experimentation and thought.

ACKNOWLEDGMENTS

The authors would like to express their appreciation to Joel Karp for assistance in data taking and reduction and to the staff of the Stony Brook accelerator laboratory for their efforts during the experiments.

*Supported in part by the National Science Foundation.

†Present address: Physics Department, University of Freiburg, Freiburg, W. Germany.

[1]J. D. Garcia, R. J. Fortner, and T. M. Kavanagh, Rev. Mod. Phys. 45, 111 (1973); Q. C. Kessel and B. Fastrup, Case Studies At. Phys. 3, 137 (1973).

[2]G. Basbas, W. Brandt, R. Laubert, A. Ratkowski, and A. Schwarzschild, Phys. Rev. Lett. 27, 171 (1971).

[3]G. Basbas, W. Brandt, and R. Laubert, Phys. Rev. A 7, 983 (1973).

[4]W. Brandt, in *Proceedings of the International Conference on Inner Shell Ionization Phenomena and Future Applications*, Atlanta, Ga., 1972, edited by R. W. Fink, S. T. Mason, J. M. Palms, and P. V. Rao

(Natl. Tech. Information Service, U. S. Dept. of Commerce, Springfield, Va., 1972), p. 948.
[5]N. Cue, V. Dutkiewicz, P. Sen, and H. Bakhru, Phys. Rev. Lett. 32, 1155 (1974).
[6]F. Hopkins, R. Brenn, A. Whittemore, N. Cue, and V. Dutkiewicz, Phys. Rev. A 11, 1482 (1975).
[7]W. Brandt and G. Lapicki, Phys. Rev. A 10, 474 (1974).
[8]J. D. Garcia, Phys. Rev. A 1, 280 (1970); 4, 955 (1971).
[9]G. S. Khandelwal, B.-H. Choi, and E. Merzbacher, At. Data 1, 103 (1969).
[10]J. R. Macdonald, L. M. Winters, M. D. Brown, T. Chiao, and L. D. Ellsworth, Phys. Rev. Lett. 29, 1291 (1972).
[11]L. M. Winters, J. R. Macdonald, M. D. Brown, T. Chiao, L. D. Ellsworth, and E. W. Pettus, Phys. Rev. A 8, 1835 (1973).
[12]J. R. Mowat, I. A. Sellin, D. J. Pegg, R. S. Peterson, M. D. Brown, and J. R. Macdonald, Phys. Rev. Lett. 30, 1289 (1973).
[13]J. H. McGuire, Phys. Rev. A 8, 2760 (1973).
[14]A. M. Halpern and J. Law, Phys. Rev. Lett. 31, 4 (1973).
[15]V. S. Nikolaev, Zh. Eksp. Teor. Fiz. 51, 1263 (1966), [Sov. Phys.–JETP 24, 847 (1967)].
[16]M. D. Brown, L. E. Ellsworth, J. A. Guffey, T. Chiao, E. W. Pettus, L. M. Winters, and J. R. Macdonald, Phys. Rev. A 10, 1255 (1974).
[17]F. Hopkins, R. Brenn, A. Whittemore, N. Cue, V. Dutkiewicz, and R. P. Chaturvedi, Bull. Am. Phys. Soc. 19, 1185 (1974).
[18]Siemens Corp., Karlsruhe, Germany.
[19]L. C. Northcliffe and R. L. Schilling, Nucl. Data 7, 233 (1970).
[20]Ortec Inc., Oak Ridge, Tenn.
[21]E. H. Pederson, S. J. Czuchlewski, M. D. Brown, L. E. Ellsworth, and J. R. Macdonald, Phys. Rev. A 11, 1267 (1975).
[22]J. R. Macdonald, P. Richard, C. L. Cocke, M. D. Brown, and I. A. Sellin, Phys. Rev. Lett. 31, 684 (1973).
[23]Cross sections of Ref. 10 have been reduced by 25% for comparison here, according to such a correction indicated in Ref. 11.
[24]R. L. Kauffman, C. W. Woods, F. F. Hopkins, D. O. Elliott, K. A. Jamison, and P. Richard (unpublished).
[25]J. A. Bearden and A. F. Burr, Nat. Bur. Stand. (U. S.) NSRDS-NBS 14 (U. S. GPO, Washington, D. C., 1967), p. 49.
[26]R. L. Kauffman, F. Hopkins, C. W. Woods, and P. Richard, Phys. Rev. Lett. 31, 621 (1973); D. L. Matthews, B. M. Johnson, L. E. Smith, J. J. Mackay, and C. F. Moore, Phys. Lett. 48A, 93 (1974).
[27]D. Burch, N. Stolterfoht, D. Schneider, H. Wieman, and J. S. Risley, Phys. Rev. Lett. 32, 1551 (1974).
[28]C. P. Bhalla, Phys. Rev. A 8, 2877 (1973).
[29]C. L. Cocke, R. R. Randall, and B. Curnutte, in *Proceedings of the Ninth International Conference on the Physics of Electronic and Atomic Collisions*, edited by J. S. Risley and R. Geballe (University of Washington Press, 1975), p. 933.
[30]J. H. McGuire and P. Richard, Phys. Rev. A 8, 1374 (1973).
[31]N. Stolterfoht, D. Schneider, and P. Ziem, Phys. Rev. A 10, 81 (1974).
[32]F. P. Larkins, J. Phys. B 4, 129 (1971).
[33]C. P. Bhalla and D. L. Walters, in Ref. 4, p. 1572.
[34]W. Bambynek, B. Crasemann, R. W. Fink, H. U. Freund, H. Mark, C. D. Swift, R. E. Prince, and P. V. Rao, Rev. Mod. Phys. 44, 716 (1972).
[35]E. J. McGuire, Phys. Rev. A 3, 587 (1971).
[36]F. Hopkins, D. O. Elliot, C. P. Bhalla, and P. Richard, Phys. Rev. A 8, 2952 (1973).
[37]L. M. Winters, J. R. Macdonald, M. D. Brown, L. D. Ellsworth, and T. Chiao, Phys. Rev. A 7, 1276 (1973); as indicated in Ref. 11, the cross sections in this reference have been reduced by 25%.
[38]R. L. Kauffman, C. W. Woods, K. A. Jamison, and P. Richard, J. Phys. B 7, 355 (1974).
[39]S. J. Czuchlewski, J. R. Macdonald, and L. D. Ellsworth, Phys. Rev. A 11, 1108 (1975).
[40]M. C. Brinkman and H. A. Kramer, Proc. Akad. Amsterdam 33, 973 (1930).
[41]S. M. Ferguson, J. R. Macdonald, T. Chiao, L. D. Ellsworth, and S. A. Savoy, Phys. Rev. A 8, 2417 (1973).
[42]J. Guffey, thesis (Kansas State University, 1974) (unpublished).
[43]R. R. Randall, C. L. Cocke, B. Curnutte, and J. A. Bednar Bull. Am. Phys. Soc. 19, 1180 (1974).
[44]D. R. Bates, in *Atomic and Molecular Processes*, edited by D. R. Bates (Academic, New York, 1962), p. 549, among others.
[45]W. L. Fite, in Ref. 44, p. 421.
[46]F. Hopkins, R. L. Kauffman, C. W. Woods, and P. Richard, Phys. Rev. A 9, 2413 (1973).
[47]J. Van den Bos and F. J. deHeer, Physica (Utr.) 34, 333 (1967).
[48]P. Richard, R. L. Kauffman, F. F. Hopkins, C. W. Woods, and K. A. Jamison, Phys. Rev. Lett. 30, 888 (1973).
[49]W. E. Meyerhof, Phys. Rev. Lett. 31, 1341 (1973).